

# Advanced simulation of CBRAM devices with the level set method

P.Dorion<sup>1,2</sup>, O.Cueto<sup>1</sup>, M.Reyboz<sup>1</sup>, J.C.Barbé<sup>1</sup>, A.Grigoriu<sup>3</sup>, Y.Maday<sup>2</sup>

<sup>1</sup> Université Grenoble Alpes CEA-LETI MINATEC, 17 rue des Martyrs, 38054 Grenoble, Cedex 9, France

<sup>2</sup> Laboratoire J.-L. Lions, Université Pierre et Marie Curie, F-75005, Paris, France

<sup>3</sup> Laboratoire J.-L. Lions, Université Paris Diderot, F-75013, Paris, France

pierre.dorion@cea.fr, Phone: +33 4 38 78 23 40

**Abstract**—A TCAD model for Chalcogenide based CBRAM is presented. This model starts from an existing model and uses an advanced level set method to follow the growth of the filament in the electrolyte. We couple the level set method with equations which model the cations migration and the electric field in the electrolyte and in the filament. We take into account silver clusters in the electrolyte in order to study their influence on switching time.

## I. INTRODUCTION

Conductive-Bridge Random-Access memory (CBRAM) is a promising technology for future nonvolatile memories, due to its low operating voltages, low power consumption and ease of integration in the back end of a logic process. A CBRAM cell is composed of a resistive switching layer encapsulated between an electrochemically active electrode, and an electrochemically inert counter electrode. The storage of the information is based on the contrast between a high resistance state and a low resistance state. Resistance switching is induced by electro-chemical driven growth and rupture of a metallic filament in the electrolyte. During write operation (SET), cations obtained from the oxidation of the top electrode migrate through the electrolyte and are reduced on the filament contributing to its growth. Starting from an existing model [1], we improve the numerical implementation of the level set method. The physical model is significantly improved by taking into account nucleation and presence of clusters in the electrolyte.

## II. PHYSICAL MODEL

### A. SET mechanisms

We study a CBRAM cell based on an active  $Ag$  top electrode, a  $GeS_2$  electrolyte and a  $W$  inert electrode illustrated by Fig. 1. Our model relies on assumptions considered in a previous model [1].

Under a sufficient positive voltage on the active electrode, the following mechanisms leading to the SET occur:

- (i) Anodic dissolution by  $Ag$  oxidation:  
 $Ag \longrightarrow Ag^+ + e^-$
- (ii) Migration of the  $Ag^+$  cations through the solid electrolyte under the action of the electric field and the gradient of concentration.

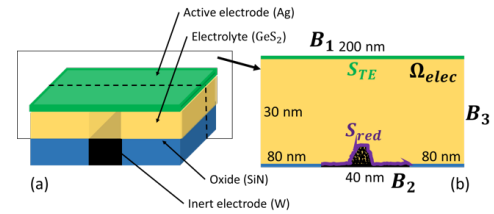


Fig. 1: a) 3D representation of study device, b) domain of resolution with the dimensions of our cell and the definition of the boundaries and reduction surface. The vector  $\vec{n}$  defines the normal at the boundary used in the expression of the boundaries conditions.

- (iii) Initialization of filaments with a nucleation mechanism occurring on bottom electrode.
- (iv) Filament growth through the reduction of  $Ag^+$  ions on filament surface according to the reaction:  
 $Ag^+ + e^- \longrightarrow Ag$ .

### B. Oxidation and reduction model

Oxidation and reduction reaction are modeled with Butler-Volmer equation which describes the electronic transfer across the electrode interface as a function of an exchange current density  $j_0$ , a charge transfer coefficient  $\alpha$  and the overvoltage  $\eta$ :

$$J_{BV} = j_0 \left( \exp \left[ \frac{\alpha e \eta}{k_B T} \right] - \exp \left[ \frac{-(1 - \alpha) e \eta}{k_B T} \right] \right) \quad (1)$$

where,  $k_B$  is the Boltzmann constant,  $T$  is the temperature and  $e$  is the elementary charge. The overvoltage  $\eta$  is the difference between electron Fermi level in the silver electrode and electron Fermi level associated to the redox couple  $Ag^+/Ag$  in the electrolyte  $GeS_2$ :

$$\eta = E_{F,Ag} - E_{f,elec} = (W_{F,Ag} + V_{ap}) - E_{redox}.$$

Neither experimental value of  $E_{redox}$  for  $Ag^+/Ag$  in  $GeS_2$  nor the experimental value of  $j_0$  are available. Consequently, these parameters are considered as adjustment parameters.

### C. Nucleation model

The initialization of the filament is obtained with the nucleation model presented by Milchev [2]. The nucleation

rate is modeled through the equation:

$$J_{nuc} = C(Z_0, N_{crit}) \exp\left(\frac{N_{crit} e |\eta_{nuc}|}{2k_B T}\right) \quad (2)$$

where  $\eta_{nuc}$  is the electrochemical overpotential. The parameter  $C(Z_0, N_{crit})$  depends on the nucleation sites number density  $Z_0$  and the number of atoms in a critical nucleus  $N_{crit}$ . Based on the nucleation rate, a stochastic algorithm is implemented on the bottom electrode surface.

#### D. Ionic drift-diffusion model

We consider space charge in our solid electrolyte is reduced to  $Ag^+$  cations and we calculate ionic concentration and electrostatic potential with the equations:

$$e \frac{\partial C_{Ag^+}}{\partial t} - \text{div}(eD\nabla C_{Ag^+} + \sigma\nabla V) = f \mathbf{1}_{bd} \quad (3)$$

$$\begin{cases} -(eD\nabla C_{Ag^+} + \sigma\nabla V) \cdot \vec{n} = J_{BV} & \text{on } B_1 \\ -(eD\nabla C_{Ag^+} + \sigma\nabla V) \cdot \vec{n} = J'_{BV} & \text{on } B_2 \\ -(eD\nabla C_{Ag^+} + \sigma\nabla V) \cdot \vec{n} = 0 & \text{on } B_3 \end{cases} \quad (4)$$

$$-\text{div}(\epsilon\nabla V) = eC_{Ag^+} \quad (5)$$

$$\begin{cases} V = V_{ap} & \text{on } B_1 \\ V = V_d & \text{on } B_2 \\ \nabla V \cdot \vec{n} = 0 & \text{on } B_3 \end{cases} \quad (6)$$

The equation (3) models the charge conservation and the Poisson equation (5) couples the electric field and the local charge density. The equation (4) and (6) define the boundaries conditions of our devices, the boundaries are illustrated by Fig. 1. The parameters  $V$ ,  $C_{Ag^+}$ ,  $\epsilon$ ,  $\sigma$  and  $D$  represent respectively the electric potential, the concentration of  $Ag^+$ , the permittivity, the conductivity and the coefficient of diffusion of  $Ag^+$ . We model the ionic conductivity with a non-linear expression of an average electric-field  $E_m = V_{ap}/H_{cell}$  in the electrolyte

$$\sigma = \frac{s_0}{E_m} \sinh\left(\frac{aeE_m}{2k_B T}\right) \quad (7)$$

where  $s_0$  is a prefactor including temperature dependency considered constant for our study,  $H_{cell}$  is the electrolyte height and  $a$  is the jump distance of the ions. Our model corresponds to a drift density of current  $\vec{j}_{Ag^+} = \sigma E$  inspired by the model of Mott and Gurney [3] for an electric field driven ion hopping.

The term  $f$  in equation (3) models the reduction on the surface of the filament and  $\mathbf{1}_{bd}$  is an interface filament-electrolyte indicator function. We consider

$$\frac{\partial}{\partial t} \int_{\Omega_{elec}} C_{Ag^+}^+ = 0 \quad (8)$$

A first approximation of (8) gives  $J'_{BV} = -\frac{S_2}{S_{TE}} J_{BV}$  and  $f = \frac{S_{fil}}{S_{TE}} J_{BV}$ .

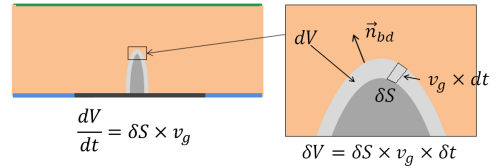


Fig. 2: Schematics of the variation of volume  $dV$  during deposition step. A spatial discretisation of this variation  $\delta V$  is expressed by considering a small surface  $\delta S$  moved during a small time  $\delta t$  at the velocity  $v_g$ .

#### E. Electrocrystallization and growth of the filament

Filament growth from critical nuclei is modeled using Faraday law which is a relation between the deposited volume and the deposition current:

$$\frac{dV}{dt} = I(t) \frac{V_{Ag}}{e} \quad (9)$$

where  $V_{Ag} = M_{Ag}/\rho_{Ag}$  is the volume of an Ag atom,  $M_{Ag}$  is the atomic mass and  $\rho_{Ag}$  is the density of Ag. The term  $I(t)$  represents the charge current through the interface. We consider the volume change, illustrated by Fig. 2, can be discretized in space by a velocity field  $\vec{v}$  which moves a little surface of the interface during a small time  $\delta t$  according to the normal of the interface  $\vec{n}_{bd}$ . The scalar product  $v_g = \vec{v} \cdot \vec{n}_{bd}$  represents the velocity of filament growth which is used in equation (4). The velocity  $v_g$  is expressed by:

$$v_g = \frac{I(t) V_{Ag}}{\delta S e} \quad (10)$$

where  $\delta S$  represents the surface moved by the velocity field  $\vec{v}$  according to the normal at the interface  $\vec{n}_{bd}$  and  $\delta t$  is the time step.

This expression of the velocity implies that the ions  $Ag^+$  which are close to the filament catch instantaneously an electron, so electron transfer is faster than mass transfer.

#### F. Silver clusters

In  $GeS_2$  electrolytes, Ag-rich clusters, known to be good ionic conductors, are observed experimentally [4] - [5]. Our model is extended by taking into account several clusters in the electrolyte. We consider that if a filament reaches a cluster, the local ionic flux increases the silver concentration inside the cluster. When a sufficient silver concentration is obtained, the cluster electrical properties ( $\epsilon$ ,  $\sigma$ ) equal those of the filament [6] and the cluster becomes an electron supplier. Nevertheless, clusters and filament chemical composition remain different and nucleation step is needed to allow restarting of filament growth.

### III. PHYSICAL MODEL NUMERICAL IMPLEMENTATION

Inside the electrolyte, the filament area corresponds to a domain with higher electrical conductivity; physical coefficients of our model have point value depending on the position in the electrolyte. We use a level set method (LSM) to define a function used to give space dependency in  $\sigma$ ,  $\epsilon$  and  $D$ .

LSM introduced by Osher and Sethian [7] is a versatile method used in many problems with an interface motion [8]. It allows including topological changes without explicit front tracking method and thus provides considerable gain in both algorithmic complexity and CPU time. This method implies a space-time function  $\varphi$  with output between 0 and 1. The interface between filament and electrolyte is defined by the level set  $\{\varphi = 0.5\}$ . The level set function  $\varphi$  is solution of an advection equation:

$$\frac{\partial \varphi}{\partial t} + \vec{v} \cdot \nabla \varphi = 0 \quad (11)$$

where  $\vec{v}$  represents the velocity of filament growth. Initialization of  $\varphi$  is obtained through the nucleation model (2) applied on the bottom electrode. When a filament reaches a cluster, cluster and filament are merged as an extension of the bottom electrode. The level set function  $\varphi$  is reinitialized from a nucleation step which occurs at the cluster surface.

#### A. Level Set Method stabilization scheme

In order to stabilize the approximation of the solution of equation (11), we adapt a stabilization scheme previously proposed by Olsson [9]:

$$\frac{\partial \varphi}{\partial t} + \text{div}(\varphi(1 - \varphi)\vec{n}) - \xi \Delta \varphi = 0 \quad (12)$$

where  $\vec{n}$  represents the normal at the interface and can be expressed by  $\vec{n} = \frac{\nabla \varphi}{\|\nabla \varphi\|}$ . These expression is not adapted in our problem because the filament is in contact with the boundary and  $\frac{\nabla \varphi}{\|\nabla \varphi\|}$  is not well defined on the boundary. We consider the normal  $\vec{n}$  is a solution of

$$\vec{n} - \chi \Delta \vec{n} = \frac{\nabla \varphi}{\|\nabla \varphi\|} \quad (13)$$

with the boundary condition

$$\begin{cases} \vec{n} = 0 & \text{on } B_1 \cup B_3 \\ \vec{n} = (f(x), 0)^t & \text{on } B_2 \end{cases} \quad (14)$$

The boundary condition is necessary to obtain the normal at the boundary with a good orientation as presented on Fig. 3. The diffusive term in equation (13) is adjusted to regularize the normal near the level set  $\varphi = 0.5$  because at the interface the normal presents numerical instabilities. As recommended by Olsson [9], we take  $\xi = h$ , where  $h$  is the characteristic mesh size. The choice of  $\chi = 10^{-17}$  results from numerical tests. The nonlinear hyperbolic equation (12) is discretized with the scheme:

$$\begin{aligned} \frac{\varphi_{k+1}^n - \varphi_k^n}{\Delta \tau} + \text{div} \left( \frac{\varphi_{k+1}^n + \varphi_k^n}{2} - \varphi_{k+1}^n \varphi_k^n \right) \\ = \xi \nabla \left( \frac{\varphi_{k+1}^n + \varphi_k^n}{2} \right) \cdot \vec{n} \text{div}(\vec{n}) \end{aligned} \quad (15)$$

In order to stabilize the solution  $\varphi^n$  at each time step, we implement equation (15) in an iterative scheme.

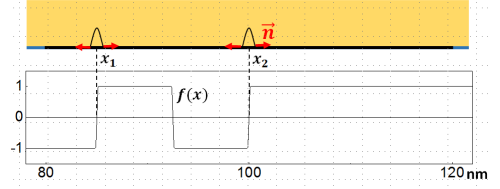


Fig. 3: Representation of  $f$  in order to obtain a good boundary condition for (13)

TABLE I: Parameters used in the simulation.

Parameter	Value	Parameter	Value
$\alpha$	0.158	$j_0$	$10^{-2} A.m^{-2}$
$T$	300 K	$a$	$7.10^{-9} m$
$s_0$	$2.10^7 A.m^{-2}$	$H_{cell}$	30 nm
$W_{F,Ag}$	-4.26 eV	$E_{redox}$	0.7996 eV
$M_{Ag}$	$1.79 \cdot 10^{-21} g.at^{-1}$	$\rho_{Ag}$	$10490 kg.m^{-3}$

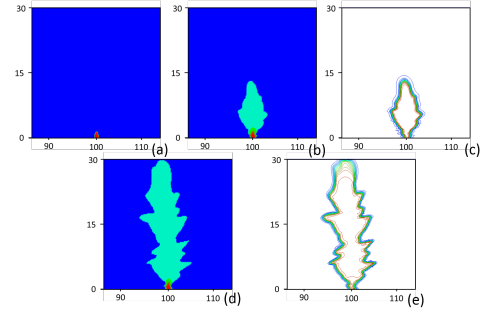


Fig. 4: Results of advection equation simulation with stabilization scheme and no clusters. (a) Initial Filament, (b) Filament at time  $t = 150ns$ , (c)  $\varphi$  at time  $t = 150ns$ , (d) Filament at time  $t = 260ns$ , (e)  $\varphi$  at time  $t = 260ns$

## IV. RESULTS AND DISCUSSION

Our model is implemented using software FreeFem++ [10]. Equations (3), (5), (12), (13) and (15) are discretized using Lagrange finite element on a cartesian mesh. The constants used in simulations are given in Tab.I. We simulate the system in a 2D domain corresponding to perpendicular cut plane of the inert electrode in a 3D structure Fig. 1.

First, we study the stabilization effect of equations (12) and (15) neglecting clusters contribution. The value of the stabilization parameters  $\xi$  and  $\chi$  are fixed by this first study. Fig. 4 illustrates the efficiency of stabilization scheme after few time steps. Please note that for long physical time, branched filament topology appears (Fig. 4d-e).

Second, we introduce clusters in the electrolyte. When the nucleation step is activated to reinitialize  $\varphi$ , we obtain one or several critical nuclei where  $\eta_{nuc}$  depending on the electrical field is stronger (Fig. 5a). From each nucleus, our model succeeds to restart filament growth in the electrolyte (Fig. 5b). The relative permittivity in the filament is chosen large enough to model electrical neutrality inside the filament (Fig. 6). The ionic conductivity and diffusivity inside cluster show constant silver concentration inside the clusters (Fig. 7).

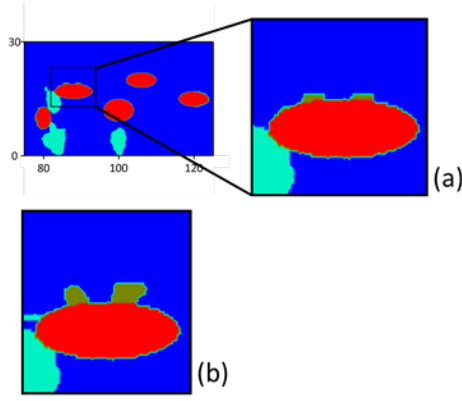


Fig. 5: (a) Reinitialization of  $\varphi$  after a nucleation step implied by clusters electrical properties changes at time  $t = 1.1\mu s$ . (b) Filament at time  $t = 1.15\mu s$ .

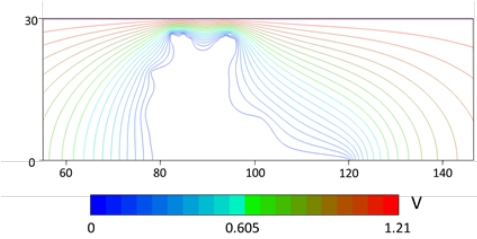


Fig. 6: Electric Potential at time  $t = 1.45\mu s$  obtained with the Poisson's equation (5) and clusters.

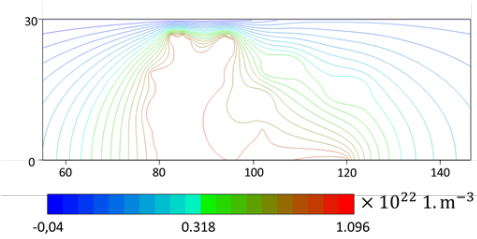


Fig. 7: Cations concentration at time  $t = 1.45\mu s$  obtained with the conservation law (3) and clusters.

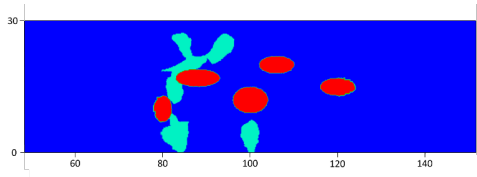


Fig. 8: Results of filament growth with clusters in the electrolyte at time  $t = 1.45\mu s$

In a 2D domain with clusters, metallic filament can connect clusters before reaching the top electrode (Fig. 8).

With the clusters inside the electrolyte, we study their effects on the time required for the filament to reach the silver electrode (switching time). Clusters are used by electrons

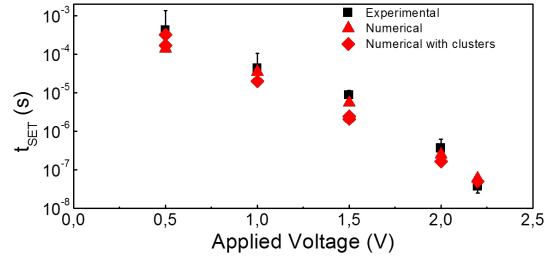


Fig. 9: Experimental and numerical switching time ( $t_{SET}$ ) for CBRAM devices with a chalcogenide ( $GeS_2$ ) electrolyte. Numerical switching time gives different results with clusters in the electrolyte.

as bridge in the electrolyte when a filament touch a cluster, so the switching time decreases (Fig. 9). The presence of clusters could explained the variability in switching time measurements.

## V. CONCLUSION AND PERSPECTIVES

We improve the level set method implementation by adjusting the normal at the interface. We improve the physical model by taking into account nucleation and Ag-rich clusters in the electrolyte. The nucleation and filament growth in a CBRAM device containing clusters can be simulated with our model. The effect of silver clusters on switching time has been studied and shows clusters change switching time.

## ACKNOWLEDGMENT

The authors would like to thank Frédéric Hecht, Charles Dapogny and Pascal Frey for fruitful discussion and for sharing FreeFem++ experience.

## REFERENCES

- [1] P. Dorion, O. Cueto, M. Reyboz, E. Vianello, J.C. Barbe, A. Grigoriu, and Y. Maday. Simulation of cbram devices with the level set method. In *SISPAD 2013*, 2013.
- [2] A. Milvhev. *Electrocrystallization Fundamentals of Nucleation and Growth*. Kluwer Academic Publishers, 2002.
- [3] N.F. Mott and R.W. Gurney. *Electronic Processes in Ionic Crystals*. Oxford, 1946.
- [4] V. Sousa. Chalcogenide materials and their application to non-volatile memories. *Microelectronic Engineering*, 88:807-813, 2011.
- [5] M.N. Kozicki, M. Mitkova, M. Park, M. Balakrishnan, and C. Gopalan. Information storage using nanoscale electrodeposition of metal in solid electrolytes. *Super. Micro.*, 34:459 - 465, 2003.
- [6] T.Z. Todorova, P. Blaise, E. Vianello, and L.R.C. Fonseca. Understanding the conduction mechanism of the chalcogenide  $ag_2s$  silver-doped through ab initio simulation. In *ESSDERC*, 2013.
- [7] S. Osher and A. Sethian. Fronts propagating with curvature dependent speed: Algorithms based on hamilton-jacobi formulations. *J. Comp. Phy.*, 79:12-49, 1988.
- [8] M.F. Gyure, C. Ratsch, B. Merriman, R.E. Caflisch, S. Osher, J.J. Zinck, and D.D. Vvedensky. Level-set methods for the simulation of epitaxial phenomena. *Phys. Rev.*, 58:6927-6930, 1998.
- [9] E. Olsson, G. Kreiss, and S. Zahedi. A conservative level set method for two phase flow ii. *J. Comp. Phy.*, 225:785-807, 2007.
- [10] F. Hecht. New development in freefem++. *J. Numer. Math.*, 20(3-4):251-265, 2012.